

CT analysis of the fracture propagation and bony damage at the interface between the distal locking screw and the cortical bone

V. GASIUNAS^{ab}, M. PROT^a, S. LAPORTE^a (14 gras)

- a. Arts et Métiers ParisTech, Institut de Biomécanique Humaine George Charpak, 151 bd de l'Hôpital, 75013 Paris,
- b. gasiunas@gmail.com

Résumé :

Le clou centromédullaire est souvent utilisé en orthopédie et traumatologie pour traiter des fractures des os longs. De meilleures connaissances des contraintes liées à l'endommagement osseux au niveau de l'interface entre la vis de verrouillage distal et l'os pourraient améliorer les techniques chirurgicales. Quarante-cinq échantillons (longueur 65mm, ϕ 20mm) prélevés au niveau de la diaphyse fémorale de brebis ont été utilisés. Des acquisitions micro scanner ont été utilisées afin d'étudier l'architecture osseuse. Des compressions quasi-statiques (1mm/s) ont été effectuées sur un barreau métallique de 4 mm de diamètre placé à l'extrémité de l'échantillon, afin de se rapprocher des conditions de la vis de verrouillage distal placé dans la région diaphyso-métaphysaire. La compression a été arrêtée à 1,5%, 3% et 6% de déformation dans trois groupes de 15 échantillons. Une nouvelle acquisition micro scanner a été faite afin d'évaluer la propagation de fracture. La force nécessaire pour fracturer l'échantillon se situe entre 2000N et 4000N. Un comportement linéaire a été observé dans la partie initiale de toutes les courbes force – déplacement ; la raideur moyenne était de 2648 ± 873 N/mm. Un comportement plastique a été observé pour 23 échantillons et la rupture complète pour 15. Dix ruptures ont été observées sans plastification. La propagation de fracture été corrélée aux différentes formes de courbes force – déplacement.

Abstract :

An intramedullary locking nail is frequently used in fracture treatment in orthopedic trauma surgery. A better understanding of strain related to bony damage occurring at the interface of the distal locking screw and the cortical bone could allow improving surgical techniques. Forty-five specimens (length 65mm, ϕ 20mm) extracted from the ewe femoral diaphysis were used in this experiment. A microCT scan was done in order to explore the initial bony architecture. Then quasi-static (1mm/s) compression was performed on a 4mm cylindrical metallic rod situated at the extremity of the specimen as to mimic the distal locking screw at the diaphysis-metaphysis area. The compression was stopped at 1.5%, 3% and 6% of strain in 3 groups of 15 specimens. Another microCT scan was done to evaluate the fracture propagation. The force necessary to induce a fracture was between 2000N and 4000N. A linear behavior was observed in the beginning of all loading curves, the stiffness was 2648 ± 873 N/mm in average. Yielding occurred in 23 and complete rupture in 15 of the 45 specimens; 10 of them without yielding. The fracture line propagation was correlated to different shapes of the curves.

Mots clefs : intramedullary nail, locking screw, microCT, fracture propagation, bony damage

1 Introduction

The intramedullary fixation is one of the most frequently used methods of osteosynthesis in the modern orthopedic and trauma surgery for long bone internal fixation [1,2].

Intramedullary fixation is a surgical technique when a metallic rod is inserted into the central canal of a long bone. There are mainly four bony segments in the human body where intramedullary nailing can be used: arm, forearm, thigh and leg. This fixation is meant to realign the bony fragments and maintain them in a wanted position until the bone heals.

In the most cases the locking screws inserted distally and proximally are used in order to ensure the suitable fixation of this intramedullary device [3]. If the fracture has a stable pattern, i.e. oblique non comminuted fracture, the longitudinal alignment would be sufficient to guarantee a good bony stability. If the fracture is comminuted and has multiple fragments, the locking device must be used in order to have a suitable longitudinal and rotational stability [4]. In such a case before the bone consolidation occurs, all the forces would go through the distal locking screw if there is any mechanical loading, e.g. walking. There are few studies analyzing the forces and strains passing through the distal locking screw and the relationships between these forces and potential bony damage.

The purpose of this study was to analyze the distal locking screw and the bone contact area in order to understand what forces are involved at this area, what is the mechanical behaviour of the distal screw and the bone under it under mechanical loading, how the bone under the distal locking screw can be damaged and what is the damage pattern if the forces come to a rupture limit.

2 Material and Methods

2.1 Specimens and Imaging

Forty-five long bone cylinders were harvested from the ewe femoral mid-shaft. The specimens measured 65mm in length and about 20mm in diameter. They were kept frozen at -20°C in a vacuum sealed plastic bags. The samples were slowly defrosted for 12 hours at +5°C before being exposed to the room temperature prior to mechanical testing. All the specimens were scanned by a μ CT (SCANCO MicroCT 100 - cubic voxel: 17.2 μ m) before and after the experimentation.

2.2 Mechanical Testing

A metallic rod with a diameter of 4mm was centrally placed on the top side each specimen in a medial to lateral direction (Fig.1a). Quasi-static compression (1mm/s) experimentations were performed using an Instron 5566. Specimens and rod were preloaded by about 1N before compressions.

Specimens were divided into 3 groups defined by the maximal displacement imposed to the rod (Table 1). Force-displacement evolutions were recorded.

Table 1: Experimental groups

	Group 1	Group 2	Group 3
Maximal displacement (mm)	0.97	1.95	3.9
Number of specimens	15	15	15
Equivalent strain (%)	1.5	3	6

2.3 Mechanical Analysis

The recorded force and displacement curves were classified into five groups: curves showing linear behavior; curves with yielding effect without rupture; curves with a total rupture with yielding; curves with a total rupture without yielding; those presenting a “double spike” shape.

The shape of the curves was analyzed in order to identify the specimens that presented yielding, total rupture, “double spike” or a combination of them. If a major rupture was identified, the further curve was discarded as it was considered not reliable.

The mechanical behavior seen in the curve was identified and assessed. Several parameters were then calculated:

- The apparent stiffness (k) for every group was calculated after having selected the middle 1/3 of the ascending part of the curve.
- The yielding (F_{yield}) was recorded where present.
- The maximal force (F_{max}) was recorded.
- The force (F_{rup}) to rupture was recorded if the rupture occurred. In the case of a “double spike” curve shape the second “spike” was taken as the F_{rup} .
- The maximal displacement (D_{rup}) to rupture was recorded in case of rupture.

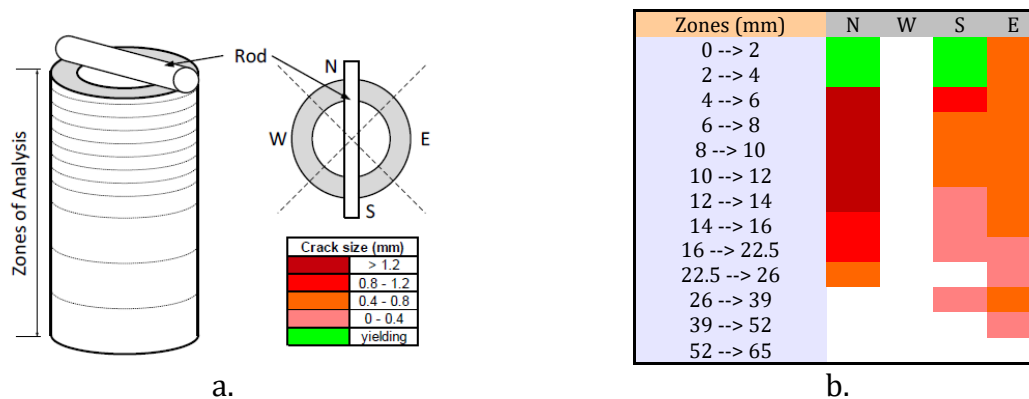


Figure 1. a) Position of the rod on the specimen and definition of zones of analysis. Colours associated with the size of crack for the pattern of damage, b) Example of pattern of rupture obtained from μ CT analysis.

2.4 Imaging Analysis

The pre and post-experimental μ CT scans were used to evaluate the shape of the specimens. In the imaging before the experimentation for a possible bony damage that might influence the mechanical behavior was looked for.

The bony damage evaluation after compression included description of yielding, fragment line propagation, an assessment of comminution at the contact area with the metallic rod and fragment migration (separation distances between the fragments). For those purposes, the cylinder of the specimen was divided into several evaluation zones. As most of the bony damage occurred at the metallic rod and the bone contact area and just below, the regions of 2mm height below the rod were created. The 2mm regions extended for 16mm, then, in order to follow the fracture line propagation the regions were expanded to 5mm down to 25mm and then – 7.5mm and 13mm (Fig.1a).

The zones were evaluated using native transversal μ CT slices taken from the middle of the evaluation zones. The image was divided into four parts that were called NESW (north, east, south, west) for identification purposes (Fig. 1a) the center coinciding with the center of the cortical bone circumference. Any comminution or bony chip was described as well as the distance between the

major fragments was measured. The distances were classified as very big (over 1.2mm), big (0.8-1.2mm), medium (0.4-0.8mm) and small (less than 0.4mm), yielding zones were identified. This evaluation allowed having a volume map of fracture propagation and its pattern in relationship with the position of the metallic rod (Fig. 1b).

2.5 Relationship between the μ CT and Mechanical analysis

The relationships between the fracture pattern and the curve groups were then studied. The attempt was made to identify the fracture pattern that could be seen as typical for the different curve type. The interdependence of the linear behavior, yielding and rupture was evaluated.

3 Results

3.1 Mechanical Analysis

A linear behavior was observed in the beginning of all the loading curves; the stiffness was quite variable, the average being $2648 \pm 873 \text{ N/mm}$ (mean \pm standard deviation).

The yielding occurred in 23 of 45 specimens, mostly in those with higher displacement (groups 2 and 3). The yielding most often started when the force was between 2500N and 3000N and usually at a displacement of 1.5mm. Only five of 23 specimens that had undergone yielding showed subsequent total rupture, all but one in the group 3.

A complete rupture occurred in 15 of 45 specimens. Ten of them occurred without an obvious yielding phase. The average F_{\max} was $3122 \pm 919 \text{ N}$, average displacement D_{\max} was $1.89 \pm 0.81 \text{ mm}$. Three of the specimens showed “double spike” curves. Then the F_{\max} for each “spike” was about 2247N. The total rupture was more frequently seen when there was no yielding effect (10 out of 15 cases of rupture).

3.2 μ CT Analysis

The μ CT analysis allowed evaluating the bony damage after the experimentation. When a total rupture was seen in a curve, the μ CT showed at least one cortical bone rupture in most cases with a longer fracture line propagation. In four of 15 specimens, the propagation line reached 58.6mm margin, 7 reached 45.5mm margin, 10 reached 32.5mm, 12 reached 15mm. Only three of 15 specimens did not show a fracture line propagation beyond 7mm and two beyond 5mm. One of them had shown some bony damage on the pre-experimental μ CT scan and was not considered reliable.

3.3 Relationship between the μ CT and Mechanical analysis

The fracture line propagation length, the fragment displacement, the two or a single cortical bone involvement was linked to different shapes of the curves (Fig.3). Most of the specimens that showed a fracture propagation line beyond 5mm had two cortical bones involved in the fracture (3 of 13 specimens). As far as different displacement groups are concerned, the most yielding curve types were observed in the group 3: 12 of 23 while there were 9 yielding types curves in the group 2 and 2 in the group 1 (Table 2).

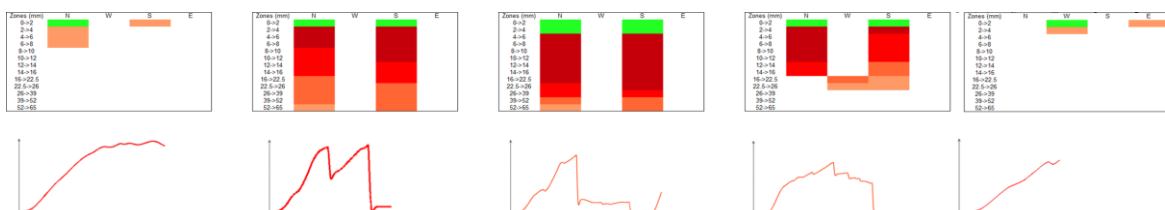


Figure 3. Imaging and mechanical behavior correlation (typical curves).

There were two complete ruptures in the group 1 (one of the specimens had some bony damage on the pre-experimental μ CT), six in the group 2 and 7 in the group 3. All the 3 specimens that had a “double spike curve had two cortical bones involved in the fracture and the propagation line went as far as the mark of 32.5mm in all of them, 45mm in 2 and 58.5mm in 1. There was much less fracture line propagation in the yielding group. The propagation line in 11 of 23 specimens that had yielding did not extend beyond 9mm and five of 23 beyond 7mm.

Table 2: Different mechanical behavior in groups. The specimens that had shown only linear linear behaviour are not included in this table.

			Group1 (N=15)	Group2 (N=15)	Group3 (N=15)	
No rupture		Number of yielding without rupture	2	8	8	Yielding
Rupture		Number of yielding with rupture		1	4	
		Number of ruptures without yielding	2	4	1	No yielding
		Number of « Double spike »		1	2	

4 Discussion

An experimental model using an animal bone was applied in this study. Although the mechanical properties depend on the age of the animal, the ewe femoral bone was chosen as it can show similar mechanical properties to the human cortical bone [5]. The specimens were frozen and thawed, but this must not have altered the biomechanical properties [6].

The μ CT scanning is an appropriate imaging for the bone damage analysis [7]. A metallic rod as a screw model was chosen for the mechanical testing in order to have less variables and thus an easier analysis of the phenomena under the rod.

Mechanical properties of the bone are close to the data found in literature [8]. The rod used instead of a screw may have limited the reproduction of the screw mechanics but has allowed simplifying the metal-bone interface and has reduced the variables that might have intervened such as the screw shape or the screw thread pattern. To mimic natural conditions the rod was placed in a lateral to medial direction at the metaphyseal area.

The linear mechanical behaviour was observed in the beginning of all curves. Double spike - the rupture of two cortical opposite bones did not occur simultaneously. It is important to note that the bony rupture occurred when the equivalent strain was 3%-6%. There were fewer fractures observed when the equivalent strain was 1.5%. This shows what strain can put the bone at risk of a fracture at the distal locking screw. Our experimental study has evaluated a single quasi-static rod compression effect on a bone. The situation can be different in a natural setting where more cyclic compressions and bone reconstruction could be observed.

The MicroCT scanning has allowed evaluating the pre-experimental bone shape and the bony damage in post-experimental scans. They have shown different fracture propagation patterns.

There were no specific studies evaluating the contact area, different forces and potential bony damage at the distal locking screw and the bone interface to the best of our knowledge. Our experimental protocol and experimental model using an animal bone allowed us to evaluate those different parameters and correlate the displacement, the forces involved and the imaging, which has allowed to get some more information about the potential bony damage at the distal locking screw.

Our protocol involved an animal bone cylinder and a metallic rod instead of the locking screw. The mechanical testing was quasi static compared to a cyclical solicitation in a clinical setting. Despite those drawbacks, our study allowed us to identify the limit values of rupture and study the bone damage patterns as the displacement of the distal locking screw comes close to the limit value of rupture.

5 Conclusion

This experimental study allowed to investigate the potential bone damage around the distal cortical locking screw of intramedullary devices by identifying several microstructural damage patterns related to the mechanical behaviour.

References

- [1] Weiss RJ, Montgomery SM, Al Dabbagh Z, Jansson KA. National data of 6409 Swedish inpatients with femoral shaft fractures: stable incidence between 1998 and 2004. *Injury*. 2009 Mar;40(3):304-8.
- [2] Yli-Kyyny TT, Sund R, Juntunen M, Salo JJ, Kröger HP. Extra- and intramedullary implants for the treatment of pertrochanteric fractures – results from a Finnish National Database Study of 14,915 patients. *Injury*. 2012 Dec;43(12):2156-60.
- [3] G.M. Whatling, L.D.M. Nokes *Injury, Int. J. Care Injured* (2006) 37, 109—119 Literature review of current techniques for the insertion of distal screws into intramedullary locking nails
- [4] Köse N, Günal I, Wang X, Athanasiou KA, Agrawal CM, Mabrey JD. Setscrew distal locking for intramedullary nails: a biomechanical study. *J Orthop Trauma*. 2000 Aug;14(6):414-9.
- [5] AI Pearce, RG Richards, S Milz, E Schneider and SG Pearce. Animal Models For Implant Biomaterial Research In Bone: A Review. *European Cells and Materials* Vol. 13. 2007 ; 1-10
- [6] Shaw J; Hunter S; Gayton, J.; Boivin, G; Prayson, M. Repeated Freeze-thaw Cycles Do Not Alter the Biomechanical Properties of Fibular Allograft Bone. *Clinical Orthopaedics & Related Research* . Mar2012, Vol. 470 Issue 3, p937-943. 7p.
- [7] Ding M, Henriksen SS, Theilgaard N, Overgaard S. Assessment of activated porous granules on implant fixation and early bone formation in sheep. *J Orthop Translat*. 2015;5:38–47. Published 2015 Oct 29. doi:10.1016/j.jot.2015.09.008.
- [8] Boughton OR, Ma S, Zhao S, et al. Measuring bone stiffness using spherical indentation. *PLoS One*. 2018;13(7):e0200475. Published 2018 Jul 12. doi:10.1371/journal.pone.0200475.